Realistic Cell and Organelle Shape Modeling for Computational Bioengineering: A New Open-Source Toolbox

Mehrdad Saviz

School of Electrical and Computer engineering
University of Tehran
Tehran, Iran
msaviz@ut.ac.ir

Reza Faraji-Dana

Center of Excellence on Applied Electromagnetic Systems
University of Tehran
Tehran, Iran

Abstract—**This paper describes a new, open-source Matlab toolbox, which can be used to directly build realistic, complex geometrical models of irregular biological cell shapes and organelles based on user definitions on single two-dimensional micrographs. The main advantages are flexibility and versatility as needed for irregular cell shape modeling for computational bioelectrical and biomechanical studies, which are not met in conventional computer modeling tools. The algorithms, results and applications are briefly described. Specifically as shown, the software can be used to study the effects of cell shape on local absorption and microthermal effects under electrical stimulation.**

Keywords- Realistic biological cell shapes, Modeling, Toolbox, Cell Biomechanics, Cell Bioelectromagnetics

I. INTRODUCTION

Interest in three dimensional geometrical modeling of cellular and sub-cellular shapes has recently increased due to a number of current research trends, and computer modeling is frequently employed for numerical simulations of the non-trivial geometrical shapes involved in bio-mechanics and bioelectromagnetics. Indeed, the necessity to consider realistic model shapes rather than traditional simple spherical approximations [1] for cells has been shown when computing the induced voltages across cell membranes [2], and recently for estimating dielectric properties of biological tissues [3] and also for chemical concentration computations[4]. The importance of computer modeling is obvious for cell morphology studies [5]. Consequently, many efforts at proper modeling of cellular shapes have been reported. A tomographic method has been reported [2] that builds 3D-models of cells using cross section images obtained by a confocal microscope and subsequent image processing. An approach based on the so-called superformula has also been adopted[6].

Need for higher flexibility and versatility in constructing irregular and curved geometries arises when many possible cell shapes and arrangements are to be simulated based on knowledge of their typical geometry, e.g. when investigating the relation between the induced fields in cells and cell shapes. It is thus desirable to develop methods that can generate typical realistic cell shapes with only modest reliance on microscopic data in a flexible, user-controlled way. Conventional geometrical modeling tools are usually tailored for industrial design, and are cumbersome for generating flexible, irregular shapes. This need has been partly addressed by Huclova et al.[6] where the "super-formula" from [7] has been investigated as a means of flexible cell modeling beyond the limitations of conventional computer-aided design/modeling (CAD) tools. However, the super-formula assumes a minimum degree of order, which makes it less useful for making realistic models of cell mitochondria, for example. Also, limitations exist when using the super-formula for modeling cell shapes that are far from regular; e.g. retinal cells.

In this paper, we present a complementary approach and its implementation as a toolbox, that can employ two-dimensional microscopy data (single micrographs) for three-dimensional model construction, and create realistic models of cells and organelles in a flexible and user-controlled way. To improve applicability, the option for generating superformula shapes has also been implemented in the toolbox. The tailored application of these algorithms to biological micrographs and their convenient use in computational modeling of cell shapes can make the modeling of many biological complex shapes easier for computational biomedical engineers and applied biologists. To the best of the authors' knowledge, no similar toolbox has yet been reported as tailored for such applications. The name SAVI stands for "Scientific Application for Visualising Irregular Cells", and its updated version is available through the website address (http://antennalab.ut.ac.ir/en/); the downloads section. The output is directly produced as a triangulated surface or voxelized model, that can be used for FEM (triangles), or Finite Difference simulations, as needed for cellular biomechanical and bioelectrical studies.

II. METHOD

Consider a two-dimensional micrograph including the cross-section of a cellular organelle in the *xy* plane. In accordance with Fig.1(a), The user can select a number of points on the boundaries of this shape, and the toolbox connects these points with arbitrary smoothness using splines. In order to build the most plausible 3D model out of the 2D curve, we shall further define an axis of rotation *O'A*. We then change coordinates to align the x-axis with *O'A*.

Angular Interpolation : This operation constitutes the principal method of creating 3D cell objects based on 2D micrographs. Denoting the two curves on either side of the axis of rotation by C_+ (y'>0) and C_- (y'<0), we define a generalized rotation around $O'x'$ which starts at C_+ with $\varphi = 0$ in the $x'y'$ plane and ends at C_- with $\varphi = \pi$. The intermediate curves at N_{samt} discrete angles of φ are instances of a gradual linear interpolation between C_+ and C_-, mapping each point on C_+ to a corresponding point on C_-. The set of curves is concatenated with itself sorted from last to first, to complete surface construction for $[0, 2\pi)$.

Angular Repetition (Periodicity) : This operation is useful in creating peripherally periodic patterns, e.g. extrusions on the surface of a white blood cell. The repetition operation can be implemented by concatenating the *set of curves* obtained in the previous section by itself N_{rep} times and compressing the whole set of curves within the angular region of $[0, 2\pi)$ with the corresponding angles $\{ \varphi_i = 2\pi i / (N_{samt} N_{rep} - 1) \; ; \; i = 1, ..., N_{rep} N_{samt} - 1 \}$.

Super-Formula Shapes: As a complementary method of three dimensional shape generation, a 3D extension [6] of the superformula (SF) [7] option has also been included in the toolbox.

Geometrical Transforms: Several conventional geometrical transforms are included that operate on 3D objects. These include *translation, rotation, scaling, centering,* and *duplication.*

Envelope: The envelope is useful for engulfing an object in a smooth vesicle, or making the outside boundaries of the outer compartment of the mitochondria, for example. It refers to the *smallest convex shape* covering an existing shape. The algorithm for constructing this minimal convex body circumscribing the 3D object (*Convex Hull*) is well known and is implemented as follows: (1) Consider the set of all points for the *original object*, (2) Construct a *Delaunay triangulation* for the set of points, (3) Detect and extract all *free faces* (faces belonging to only one tetrahedral element.) The faces thus obtained constitute the boundary surface of the envelope.

Triangulation: Consider all intermediate curves C_i to have the same number of points.

It follows that one can define all the edges by establishing connections in the set of points $P_{n,i} = \left(x_{n,i}^{3d}, y_{n,i}^{3d}, z_{n,i}^{3d} \right)$ as
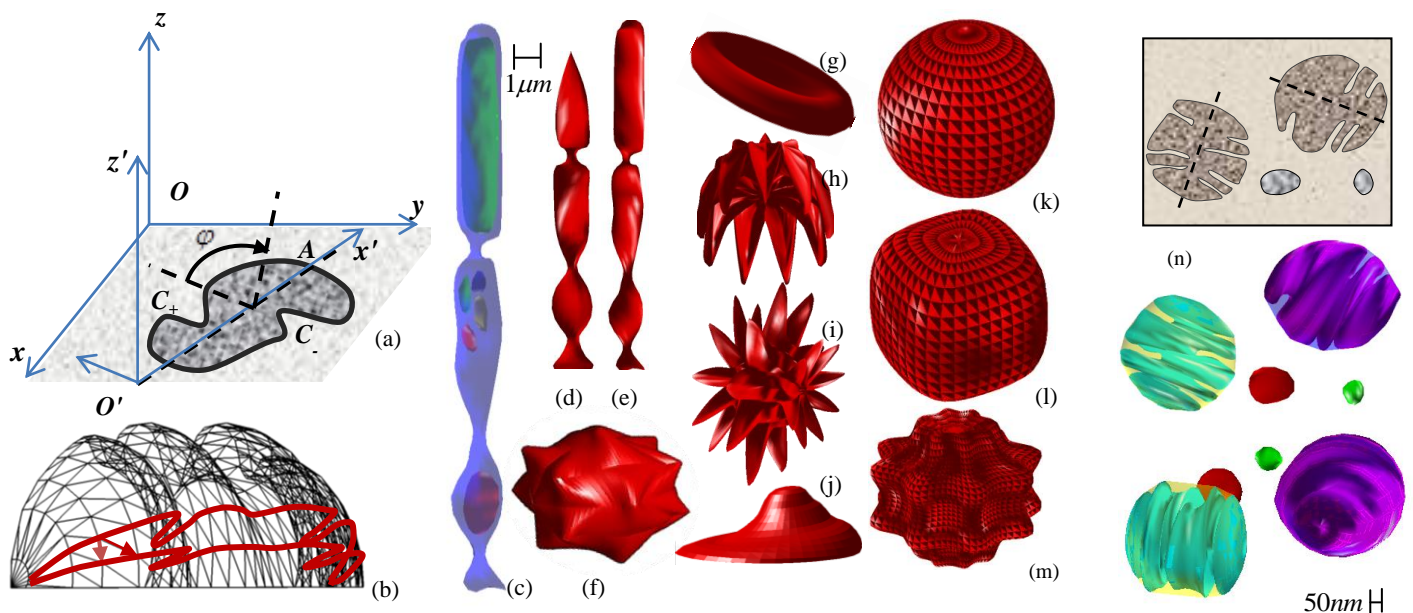

Fig.1. (a) The generalized rotation, consisting of interpolating between the curves on either side of the axis O'A. (b) mesh generation. Two curves are highlighted in red. Small arrows depict the connection scheme to define triangle edges. Examples of generated cell shapes are shown in (c) a rod cell with filled outer segment and several mitochondria, and a nucleus. (d,e) cone and rod cells, (f) *echinocyte* and (g) normal red blood cell, (h) *horizontal cell* in the retina, (i) small white blood cell, (j) flattened cell in culture plate, and (k-m) super-formula generated shapes: (k) spherical cell, (l) cuboidal cell, and (m) cell with protrusions. The $1\mu m$ scale-bar refers to (c), which is a transparent magnified version of (e). (n) Mitochondria models, from two different angles. The 2D sketch is redrawn from electron microscope images, whose sources can be found at http://remf.dartmouth.edu/images/mammalianLungTEM/.

$P_{n,i} \rightarrow P_{n,i+1}$, $P_{n,i} \rightarrow P_{n+1,i+1}$. for all possible i and n. Also, the first and points on each curve form edges by connecting to a point on the axis of rotation. This procedure is illustrated in Fig. 1(b). The areas between the edges form the triangles that cover the face of the 3D object.

Output Formats: There are currently three conventional export formats for objects created in the toolbox. The first is the conventional STL format which describes the surface of the 3D object as a set of triangular patches. For this operation, the open-source code *stlwrite.m* [8] has been used with no modification. The second choice is a volume description of the objects with voxels (volume cells). Each object is converted to an m-by-n-by-p binary valued array indicating wether each grid point is inside (binary value:1) or outside (binary value:0) the object. The open-source code *voxelise.m* [9] has been used for this operation. Finally, a conventional faces-vertices structure as appropriate for use in MATLAB can be chosen.

III.   RESULTS AND DISCUSSION

In order to provide an overview of the practicality and applications of the modeling toolbox, we present geometrical models for several types of complex, irregular cells. We also provide an example of computational microdosimetry using the generated cell models.

Modeling complex cell shapes

The cell models in Fig.1 have been obtained based on knowledge obtained from several micrographs. For the rod and cone cells, by keeping the relative position in 3D in accordance with those of the 2D plane, the toolbox enables flexible inclusion of organelle details in arbitrary places inside the cell. The mitochondria model uses an envelope to produce the outer compartment. These models can be readily used for simulations within commercial software modules.

Computational Microdosimetry

Using the proposed toolbox we have modeled the induced currents within the cytoplasm of a retinal rod cell under the influence of low frequency electric fields. Rod cells, are considered to be composed of four main parts: the outer segment (which incorporates light-sensitive proteins), the inner segment containing the metabolic organelles, the nucleus, and a synaptic region [10].

The structure and fine modeling details of retinal rod cells are described previously by the authors [11]. Here we concentrate on the realistic modeling of the 3D structure and the corresponding field results.

The cell model created using the introduced toolbox is shown in Fig. 2. Such model can be built on the basis of
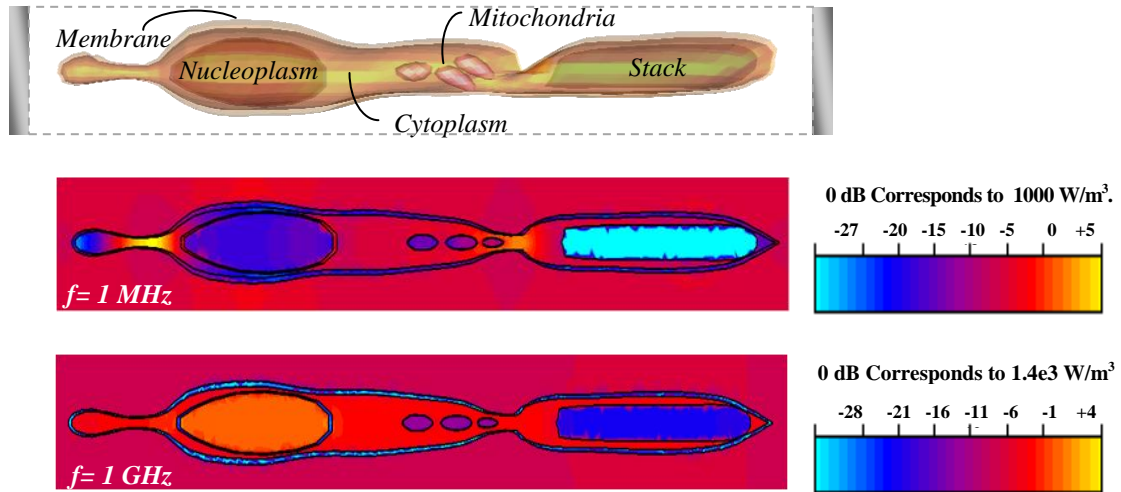

Fig.2. Example simulation: The generated 3D cell model and volume density plots of heat generation within the cell for exposure to 1MHz and 1GHz electric fields. Excitation field vector is along the cell axis and has been simulated by applying an electric field of 77 V/m between the two electrodes, distanced 36 μm apart. Realistic, frequency-dependent dielectric and conductivity properties used for the models are from references [11-13] and are as follows, for f = 1MHz, and f= 1GHz respectively: $\varepsilon_{cytoplas} = 184,64$, $\sigma_{cytoplasm} = 0.4, 1.17$ S/m, $\varepsilon_{Membrane} = 12.8, \sigma_{Membrane} = 5.6 \times 10^{-5}$ S/m, $\varepsilon_{Ex.Cellular} = 48,47.9$, $\sigma_{Ex.Cellular} = 0.3, 0.4$ S/m, $\varepsilon_{Nucleoplasm} = 90, 61.6, \sigma_{Nucleoplasm} = 2.8, 3.6$ S/m, $\varepsilon_{Nuc.Envelope} = 160, \sigma_{Nuc.Envelope} = 0.011$ S/m, $\varepsilon_{Stack} = 18, \sigma_{Stack} = 10^{-6}$ S/m,   and $\varepsilon_{Mito} = 54, \sigma_{Mito} = 0.12$ S/m.

micrographs [10]. The whole cell has a diameter of about 1.7 μm and a total length of about 30 μm. To compute the electric field distribution within the cell, the model is excited by placing the cell between two electrodes, filled with material properties of physiological saline, in the commercial electromagnetic simulator CST EMS®. Tangential boundary conditions on the four lateral sides correspond theoretically to two-dimensional periodicity of the model. Consequently, the effect of adjacent cells on the field distribution are taken into account. The absorption distribution for selected radio and microwave frequencies are given in the caption of Fig.2. An important observation is the possible current-driven amplification within the synaptic "neck". The loss density at this region is seen to be 20 times higher than the ambient loss within the tissue (represented by the extracellular medium ECM and most of the cytoplasm). This effect can be understood as current amplification, which occurs when free-charge currents have to pass through a smaller passage in series with a larger one, surrounded by poorly conducting cell membranes. This type of amplification relaxes at higher frequencies, where displacement current become dominant relative to free-charge (ionic) currents, as can be seen in the results for f= 1GHz.

IV. CONCLUSION

We have described a set of geometric design tools that we have found useful in generating realistic cellular and sub-cellular shapes and for composing 3D models out of 2D microscopic images. We have also reported an open source, flexible toolbox with a user-friendly graphical user interface which incorporates all the tools introduced. These tools find application in numerical modeling for solving problems in computational bioelectromagnetics and microdosimetry. They produce various smooth shapes that are not as easily generated by the conventional industrially-optimized CAD tools.

ACKNOWLEDGMENT

REFERENCES

[1] J. L., Munoz, S. Sebastian, M. Sancho, and J. M. Miranda, "Analysis of the influence of the cell geometry, orientation and cell proximity effects on the electric field distribution from direct RF exposure," *Phys. Med. Biol.* , vol. 46 , pp. 213–225, 2001.

[2] G. Pucihar, T. Kotnik, B. Valič, D. Miklavčič, "Numerical Determination of Transmembrane Voltage Induced on Irregularly Shaped Cells," *Annals of Biomedical Engineering,* vol. 34, no. 4, pp. 642-52, 2006.

[3] S. Huclova, D. Erni, and J. Fröhlich, "Modelling and validation of dielectric properties of human skin in the MHz region focusing on skin layer morphology and material composition ," *J. Physics D: Applied Physics* , vol. 45, p. 025301., 2012.

[4] H. W. Choi, A. I. Barakat, "Modulation of ATP/ADP Concentration at the Endothelial Cell Surface by Flow: Effect of Cell Topography," *Annals of Biomedical Engineering.*, vol.37(12), pp.2459-68 ,2009.

[5] K. Khairy, J. Foo, and J. Howard, "Shapes of Red Blood Cells: Comparison of 3D Confocal Images with the Bilayer-Couple Model," *Cellular and Molecular Bioengineering*, vol. 1(2–3), pp.173–81, 2008.

[6] S. Huclova ,D. Erni, and J. Fröhlich, "Modelling effective dielectric properties of materials containing diverse types of biological cells," *J. Phys. D: Appl. Phys.* vol.43, p.365405, 2010.

[7] J. Gielis, "A generic geometric transformation that unifies a wide range of natural and abstract shapes," *Am. J. Bot.*, vol. 90, no. 3, pp. 333-38, 2003.

[8] Sven. (2012, August) stlwrite - Write binary or ascii STL file. [Online]. http://www.mathworks.com/

[9] Aitkenhead A.H. (2010, May) Polygon mesh voxelisation. [Online]. http://www.mathworks.com/

[10] H Lodish et al., Molecular Cell Biology.: W. H. Freeman & Company, 2003.

[11] A. Molaei, M. Saviz, and R. Faraji-Dana, "Detailed modeling and numerical analysis of photoreceptor cells exposed to electromagnetic waves," Proceedings of the Iranian Conference on electrical Engineering,Tehran, 2011.

[12] R P Joshi, Q Hu, and K H Schoenbach, "Modeling studies of cell response to ultrashort, high-intensity electric fields- impications for intracellular manipulation," *IEEE Trans. Plasma Sci.* , vol. 32, pp. 1677-86, 2004.

[13] J. Gimsa, T. Müller, T. Schnelle, G. Fuhr, "Dielectric Spectroscopy of Single Human Erythrocytes at Physiological Ionic Strength: Dispersion of the Cytoplasm," *Biophys. J.*, vol. 71, pp.495-506, 1996.